Applied Thermal Engineering 103 (2016) 56–66

Contents lists available at ScienceDirect

Applied Thermal Engineering

journal homepage: www.elsevier.com/locate/apthermeng



Research Paper

# Cost optimisation of supermarket refrigeration system with hybrid model

Miha Glavan [a,*], Dejan Gradišar [a], Serena Invitto [c], Iztok Humar [b], Đani Juričić [a], Cesare Pianese [c], Damir Vrančić [a]

[a] Department of Systems and Control, Institut "Jožef Stefan", Jamova 39, 1000 Ljubljana, Slovenia
[b] Faculty of Electrical Engineering, University of Ljubljana, Tržaška 25, 1000 Ljubljana, Slovenia
[c] Department of Industrial Engineering, University of Salerno, Giovanni Paolo I, 84084 Fisciano, SA, Italy

## HIGHLIGHTS

- A procedure for modelling the refrigeration system is presented.
- Temperature dynamics of display case and food products are estimated.
- Modelled discrete events consist of door openings, food refiling and defrosting.
- Several optimisation measures of store-wide refrigeration system are evaluated.
- Operational costs and food quality degradation are taken into consideration.

## ARTICLE INFO

*Article history:*
Received 22 January 2016
Accepted 30 March 2016
Available online 19 April 2016

*Keywords:*
Refrigeration system modelling
Thermodynamics
Discrete events
Agent-based model
Optimisation

## ABSTRACT

Refrigeration systems based on vapour compression cycle are one of the largest energy consumers in supermarkets. In this paper a hybrid model of a refrigeration system is developed, in order to estimate the benefits of energy optimisation measures. The refrigeration model comprises the refrigerated display case dynamics, food products dynamics, evaporation model, and ice formation model, and is further extended with the discrete events that are typical for normal operation of a refrigeration system (i.e. customer interactions, product refilling, defrosting). Model parameters are identified from the measured data, equipment specifications and estimations of some conditions in a supermarket case study. The simulation software AnyLogic is used to realise an agent-based model of the display case that allows us to extend the model to the entire store-wide refrigeration system. The analysis demonstrates the use of the model for system optimisation purposes. The defrosting schedule of a single display case as well as for the complete store is optimised considering the overall running costs, food quality, and maximum peak power. Moreover, several energy optimisation measures are compared and evaluated in terms of their contribution to the overall savings and food quality degradation.



## 1. Introduction

Energy related costs represent a major part of the total costs of retail companies. The energy consumption is large due to the need to maintain a comfortable and stable environment for customers, employees, and products on display. They need to provide sufficient artificial lighting, a comfortable temperature, and ventilation.

The most typical and also the largest energy consumer in supermarkets are the refrigeration systems, which can typically consume up to 40% of the total energy [1]. Therefore, refrigeration systems usually have great potential for optimisation. According to the survey presented in [2], several energy minimisation strategies exist. They extend from the rather simple and trivial measures of increased insulation, regular maintenance, air infiltration protection, new equipment installation, etc., to actions that require more complex approaches, like the optimisation of defrosting and the modification of the control. Narrowly focused refrigeration optimisation approaches are also being applied, where the focus is on a specific component of the refrigeration system (e.g. the evaporator [3] or the condenser [4]). In contrast, some holistic approaches are examined, where the interaction or even integration of HVAC and the refrigeration system is considered [5]. In addition,

* Corresponding author.
*E-mail address:* miha.glavan@ijs.si (M. Glavan).

http://dx.doi.org/10.1016/j.applthermaleng.2016.03.177
1359-4311/

**Nomenclature**

| | |
|---|---|
| $T$ | temperature (°C) |
| $\dot{Q}$ | heat transfer rate (W) |
| $UA$ | heat transfer coefficient times contact area (W/K) |
| $c_P$ | specific heat capacity (J/kg K) |
| $m$ | mass (kg) |
| $\dot{m}$ | mass flow (kg/s) |
| $\dot{V}$ | volume flow (kg/s) |
| $\rho$ | density (kg/m$^3$) |
| $p$ | pressure (Pa) |
| $P$ | power (W) |
| $k_{v,max}$ | valve capacity (m$^3$/s) |
| $u_v$ | opening degree of valve (%) |
| $\Delta h_{lg}$ | specific latent heat (J/kg) |
| $h$ | enthalpy (J) |
| $x$ | specific air humidity ($kg_{water}/kg_{air}$) |
| $g$ | gravitational constant (m/s$^2$) |
| $A$ | non-blocking area (m$^2$) |
| $H$ | height of area (m) |
| $k_{fr}$ | degradation rate (m$^3$/($kg_{water}$ s)) |
| $\eta_{mes}$ | overall mechanical, electrical and isentropic efficiency |
| $\eta_e$ | evaporator efficiency |
| $\delta$ | discrete door-opening event |
| $\lambda$ | exponential distribution rate |
| $Thr_m$ | triangular distribution mode |
| $c_e$ | energy tariff |
| $z$ | product sensitivity |
| $D_{T,ref}$ | quality loss factor |
| $t_{start}$ | defrost start time |
| $t_d$ | defrost time delay |

*Subscripts*

| | |
|---|---|
| $f$ | food surface |
| $c$ | core |
| $w$ | wall |
| $a$ | air |
| $e$ | evaporator |
| $r$ | refrigerant |
| $s$ | store |
| $h$ | defrost heater |
| $suc$ | suction manifold |
| $cnd$ | condensation |
| $comp$ | compressor |
| $fr$ | frost |
| $akv$ | expansion valve |
| $ref$ | refrigerator |
| $i$ | input |
| $is$ | isentropic |
| $PI$ | proportional–integral control |

sophisticated cost reduction strategies are being introduced lately, where the thermal storage of refrigeration systems is employed to realise various demand response action schemes (e.g. [6,7]).

Refrigeration system modelling represents the most widely adopted approach to achieve better system design to optimise the energy consumption of the systems. The developed space-distributed models usually focus on a geometry-specific analysis that is focused on the optimisation of some refrigeration component or even complete refrigerated display case system (e.g. [8,9]). Data-based models are convenient for extending the analysis to a complete refrigeration system that is comprised of several parallel display cases. Such models exploit logged store data, and enable faster ways to deploy a model with sufficient performance [10–12]. The true usefulness of such statistical models is however severely limited in cases where the extrapolation of the system dynamics is needed. The most widely applied store-wide refrigeration system models are therefore described with first principles, where basic thermodynamic relations are considered [13–19]. These models combine relative model simplicity with a physical foundation, that can be tuned for each specific case.

Another important aspect when considering refrigeration system performance are the discrete events. These are mainly the consequence of random human interaction with the display case, whilst others are the consequence of scheduled or non-scheduled refrigeration actions. Discrete event models of refrigeration systems are rarely applied, or are commonly limited to door opening events [20].

The majority of the refrigeration optimisation research literature is focused solely on the minimisation of the overall operating costs. But in reality, the unstable and also hazardous nature of the refrigerated products should be taken into account. A multi-objective approach is needed, where food degradation is also controlled. The quality performance index should directly follow the HACCP standards for refrigerated food that specifies the temperature limits. This is typically implemented with an index that is proportional to the violations of the limits [21,22].

In this article a complete refrigeration system model is developed. The identified first-principle model is upgraded with typical discrete events (defrosting, product refilling, customer's interaction). The model can be updated to reflect the conditions of the specific supermarket and enables optimising the system settings and comparing different optimisation strategies. The considered actions can be also extended to the level of social behaviour, where the influence of the customers and shop personnel can be examined. With the proposed tool it is possible to find out what are the expected benefits of potential optimisation strategies in the sense of the overall refrigeration costs and the underlying quality of the food.

This paper is organised as follows. In the next section the refrigeration model is introduced, where the main focus is on the presentation of dynamic and discrete-event models, and the identification of the model parameters for the considered case study. Section 3 presents the optimisation framework and the results of the case study optimisation. Lastly, the conclusions are presented in Section 4.

## 2. Modelling refrigeration systems

The most common refrigerators and freezers have four major parts in their refrigeration system: compressor, condenser, expansion valve, and evaporator. In the evaporator section, a refrigerant is vaporised to absorb heat added into the refrigerator due to heat transfer across the refrigerators walls and convection through the door, seals and during door opening. The evaporator temperature is maintained at, or near, the refrigerant boiling temperature. In the next stage, an electric motor runs a piston compressor and the refrigerant is pressurised. This raises the temperature of the refrigerant and the resulting superheated, high-pressure gas (it is still a gas at that point) is then condensed to a liquid in an air-cooled condenser. Supermarket refrigeration systems usually apply common compressor and condenser coils for several refrigerators. From the condenser, the liquid refrigerant flows through an

expansion valve, in which its pressure and temperature are reduced and these conditions are maintained in the evaporator. The whole process operates continuously by transferring heat from the evaporator section to the condenser section by pumping refrigerant continuously through the system described above.

The costs of commercial refrigeration system operation are in general affected by two main factors: the technological overall efficiency of the appliances and the losses due to interactions with the system (customers and the shopping centre's personnel). For a single refrigerator, the most influential variables determining the energy costs are: defrosting the evaporator's coil, filling the refrigerators with new products, the opening of refrigerator doors by the customers, etc.

A dynamical model that would take into account also various discrete events is needed, in order to evaluate and compare all these effects. The following subsection introduce the developed model. First a single display case model that consists of a dynamical part and a discrete-event part is described. Then this model is extended to the store-wide level of several display cases. The simulation software AnyLogic [23] is used for modelling, as it supports various simulation methodologies, i.e. System Dynamics, Discrete Events and Agent Based Modelling.

### 2.1. Dynamical model of a display case

The dynamical model of a refrigerated display case consists of three main parts: display case model, evaporation model, and ice formation model. The first part describes the temperature dynamics of the display case, the second part relates the refrigerant mass flow to the refrigeration heat flow, and the last part formulates the deterioration effects of the ice formation process.

A low temperature display case, located in one of the local shopping centres, was chosen as a case study. The model parameters were selected according to the equipment specifications, field measurements, and additional data acquired from the refrigeration system.

#### 2.1.1. Display case model

The temperature dynamics of the display case are directly related to the underlying thermodynamical equations. The model structure was inspired by the articles [16–18], where a simplified structure of the display case was applied. Here, a model with 7 heat flows is adopted, as shown in Fig. 1.

The following variable nomenclature is used to describe the refrigeration dynamics: $T$ denotes the temperature, $\dot{Q}$ represents the heat flow, $UA$ represent the overall heat transfer coefficient ($U$) multiplied by the contact area ($A$); and the indices are $f$ (food surface), $c$ (core), $w$ (wall), $a$ (air), $e$ (evaporator), $r$ (refrigerant) $s$ (store) and $h$ (defrost heater). In reality, the heat capacity of the air is close to zero. To reduce the complexity of the model and to avoid consequent numerical problems, it is additionally assumed that the air dynamics is very quick and that the following static relation completely determines the refrigerated air temperature [18]:

$$T_a = \frac{T_f \cdot UA_f + T_w \cdot UA_w + T_e \cdot UA_e}{UA_f + UA_w + UA_e} \tag{1}$$

Linear heat transfer dynamics can be represented with a state-space representation. The states $x$ consist of the main display case temperatures $(T_f, T_c, T_w, T_e)$. The output vector $y$ is selected according to the available measured data $(T_f, T_c, T_a, T_e)$, and the input vector $u$ consists of the store temperature, the defrost heater heat flow, and the evaporator heat flow $(T_s, \dot{Q}_h, \dot{Q}_r)$. The state-space representation of the model is

$$\dot{x} = Ax + Bu \tag{2}$$

$$y = Cx \tag{3}$$

where the matrices $A, B, C$ are

$$A = \begin{bmatrix} \frac{-UA_f - UA_c}{m_f c_{pf}} + \frac{UA_f^2}{m_f c_{pf} UA_{tot}} & \frac{UA_c}{m_f c_{pf}} & \frac{UA_f UA_w}{m_f c_{pf} UA_{tot}} & \frac{UA_f UA_e}{m_f c_{pf} UA_{tot}} \\ \frac{UA_c}{m_c c_{pc}} & \frac{-UA_c}{m_c c_{pc}} & 0 & 0 \\ \frac{UA_w UA_f}{m_w c_{Pw} UA_{tot}} & 0 & \frac{-UA_w - UA_s}{m_w c_{Pw}} + \frac{UA_w^2}{m_w c_{Pw} UA_{tot}} & \frac{UA_w UA_e}{m_w c_{Pw} UA_{tot}} \\ \frac{UA_e UA_f}{m_e c_{Pe} UA_{tot}} & 0 & \frac{UA_e UA_w}{m_e c_{Pe} UA_{tot}} & \frac{-UA_e}{m_e c_{Pe}} + \frac{UA_e^2}{m_e c_{Pe} UA_{tot}} \end{bmatrix} \tag{4}$$

$$B = \begin{bmatrix} 0 & 0 & 0 \\ 0 & 0 & 0 \\ \frac{UA_s}{m_w c_{Pw}} & 0 & 0 \\ 0 & \frac{1}{m_e c_{Pe}} & \frac{-1}{m_e c_{Pe}} \end{bmatrix} \tag{5}$$

$$C = \begin{bmatrix} 1 & 0 & 0 & 0 \\ 0 & 1 & 0 & 0 \\ \frac{UA_f}{UA_{tot}} & 0 & \frac{UA_w}{UA_{tot}} & \frac{UA_e}{UA_{tot}} \\ 0 & 0 & 0 & 1 \end{bmatrix} \tag{6}$$

and $UA_{tot} = (UA_f + UA_w + UA_e)$ is introduced to simplify the notation.

In order to conform the model to the dynamics of the considered display case, model parameters have to be identified. Identification dataset consisted of the defrosting events, as these events represent the most informative data portions, where significant temperature changes occur. A data logging system was implemented to capture the real temperature dynamics (i.e. $T_f, T_c, T_a, T_e$). Moreover, the energy flows $(\dot{Q}_h, \dot{Q}_r)$ during defrosting periods were determined from the evaporator and heater specifications.

Prior to the identification, an assumption was made that in steady state the wall temperature equals the mean of the store temperature and the refrigerated air temperature (i.e. $UA_w$ equals $UA_s$). Moreover, the number of products was assumed constant for all defrost cases, and the core food mass was estimated from the situation of the average display case ($m_c = 120$ kg).

External measurement system was installed into the display case to obtain more detailed on-field measurements. Fourteen defrost periods were recorded with sampling times of 10 s (external measurement system – $T_a, T_c, T_f$) and 15 min (display case measurements – $T_e$). Data interpolation was applied for $T_e$, in order to conform to 1 min sampling time for all data.

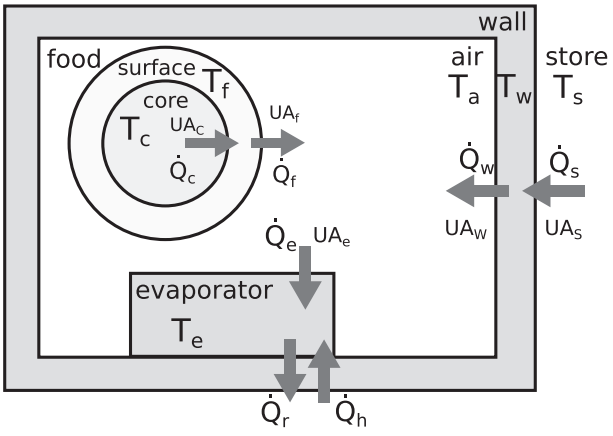


**Fig. 1.** Thermodynamical part of the model.

**Table 1**
Identified parameters of dynamical model of refrigeration.

| Parameter | Identified value | Unit |
|---|---|---|
| $UA_f$ | 143.9 | W/K |
| $UA_c$ | 53.48 | W/K |
| $UA_w, UA_s$ | 32.44 | W/K |
| $UA_e$ | 214.3 | W/K |
| $m_w$ | 50.1 | kg |
| $m_e$ | 165.2 | kg |
| $m_f$ | 13.69 | kg |

Half of the dataset was used to identify the free model parameters. Parameters were identified by the prediction error minimisation approach utilised by the *greyest* function in Matlab System Identification Toolbox. Additionally, output weighting was applied to decrease the importance of the interpolated measurements of the output $T_e$ within cost function. The identified values of the model parameters are shown in Table 1. Note, that unmodelled system dynamics is reflected within some of the identified model parameters. For instance, assumption of static refrigeration air equation is partly reflected in higher identified value of the evaporator's mass.

Validation responses of the remaining defrosting events, that were not used for identification, are represented in Fig. 2. Model predictions show a good match concerning the available temperature measurements. Due to overall food mass variation in the refrigerator, that has not been measured, some temperature offset is noticed for $T_c$ predictions. More extreme deviation can be noticed for high $T_e$, but also this could be expected in advance, as in reality the interpolation of scarce $T_e$ measurements significantly deviate from the real temperatures due to relatively quick dynamics of defrost phase.

### 2.1.2. Evaporation model

The refrigerant cycle consists of three main parts: the expansion valve, the evaporation coils, and the compressor.

Opening of the valve $u_v$ determines the refrigerant mass flow, which can be evaluated with the following equation [24]:

$$\dot{m}_{r,akv} = u_v \cdot k_{v,max} \cdot \sqrt{\rho_r (p_{cnd} - p_{suc})} \tag{7}$$

where $k_{v,max}$ is the maximal expansion valve coefficient obtained from the valve specifications [25] and $\rho_r$ denotes the density of the refrigerant. The variables $p_{suc}$ and $p_{cnd}$ are the pressures in the suction manifold (after the evaporator) and in the display case

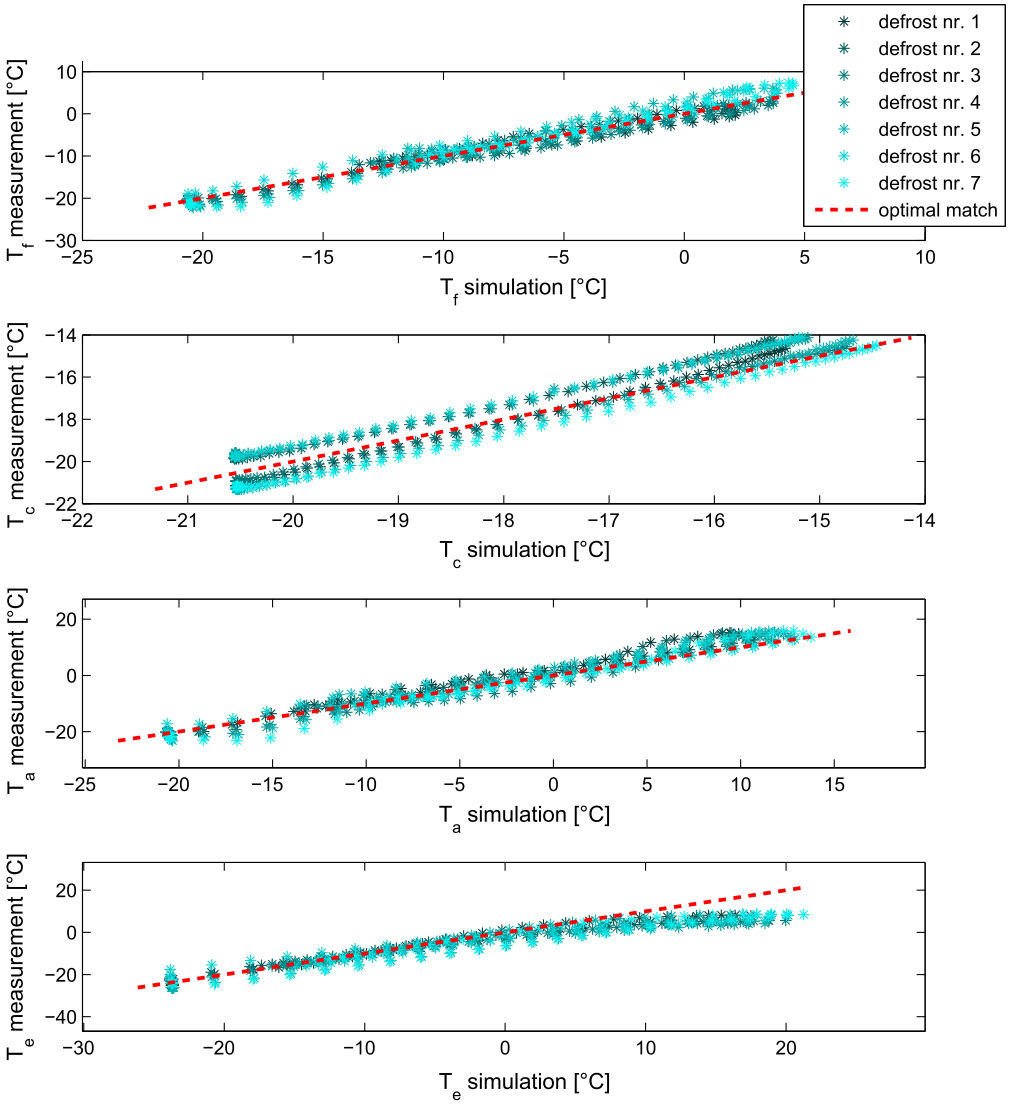


**Fig. 2.** Evaluation of the dynamical refrigeration model on the testing dataset.

conduit (before the expansion valve), respectively. The enthalpy change of the refrigerant ($\Delta h_{lg}$) and the refrigerant mass flow determines the heat flow due to the evaporation of the refrigerant [16]:

$$\dot{Q}_{akv} = \Delta h_{lg} \cdot \dot{m}_{r,akv} \tag{8}$$

The expansion valve is controlled to reach the desired refrigeration temperature in the cabinet. A PI controller is applied to maintain the appropriate valve opening, where $u_{v,PI} = 0$ represents a completely closed valve and $u_{v,PI} = 1$ denotes a completely opened valve.

In cases when the maximal heat transfer of the evaporator is lower than the current refrigerant heat transfer, the opening of the evaporator needs to be limited. In these cases the local superheat controller should decrease the valve opening in order to keep the refrigerant completely vaporised within the evaporator. Resulting valve opening is defined as:

$$u_v = min\left(u_{v,PI}, \frac{\dot{Q}_{r,max}}{\dot{Q}_{akv(u_v=1)}}\right) \tag{9}$$

where $\dot{Q}_{r,max} = UA_r(T_r - T_e)$ determines the maximal achievable heat transfer between the evaporated refrigerant in the coils ($T_r$) and the evaporator's surface ($T_e$). A constant heat transfer coefficient ($UA_r$) is assumed, as the refrigerant mass dynamics has not been directly modelled due to very fast mass dynamics which significantly increased the simulation complexity [18].

Display cases in supermarkets are usually connected to the central piping system where one stack of compressors covers several display cases. In such a centralised system it is difficult to evaluate the proportion of the electric consumption for one display case, as the working point and also the number of the running compressors changes according to the current refrigerant demand. For this reason, the evaluation of the compressor's power consumption was simplified: a constant working point is assumed and the current power consumption is evaluated with the work needed to change the enthalpy of the refrigerant that flows through the evaporator of the considered display case:

$$P_{ref} = \frac{1}{\eta_{mes}} \dot{m}_{r,akv}(h_{is,comp} - h_{i,comp}), \tag{10}$$

where $\eta_{mes}$ is the overall mechanical, electrical and isentropic efficiency and $h_{is,comp}$ and $h_{i,comp}$ are the isentropic enthalpy of the refrigerant at the output of the compressor and enthalpy of the refrigerant at the input of the compressor, respectively.

To determine refrigerant dependent variables (i.e. $\rho_r, \Delta h_{lg}, T_r, h_{is,comp}, h_{i,comp}$) a nonlinear characteristics of the R404A refrigerant were considered [26]. A fixed working point was based on mean values, measured on the refrigeration system used as a case study – superheat temperature: 6.7 °C, temperature of the refrigerant at compressor input: −1.15 °C, suction pressure ($p_{suc}$): 1.65 bar, condensation pressure ($p_cnd$): 16.23 bar. In our case, where alternative optimisation measures are directly compared, it is reasonable to assume a fixed working point. But if changes of the outside temperature and compressor or condenser dynamics need to be considered, a model should be upgraded and linearised characteristics of the refrigerant need to be taken into account.

### 2.1.3. Ice formation model

As the evaporator is continuously exposed to the moist air, frosting of the evaporator's coils occurs. The fan air flow through the evaporator is decreased by frost growth, which is the main cause for a decreased evaporator cooling capacity and consequently a reduced overall refrigeration efficiency [27]. A simple model was employed to describe the relation between the ice formed and the evaporator's cooling capacity. The mass of the ice ($m_{fr}$) formed on the coils of the evaporator depends on the air flow from the store ($\dot{m}_{a,in}$) and the difference between the specific air humidity in the store ($x_{a,s}$) and in the refrigerator ($x_{a,ref}$):

$$\dot{m}_{fr} = \dot{m}_{a,in}(x_{a,s} - x_{a,ref}) \tag{11}$$

The air flow consists of two parts: a constant part $\dot{m}_{a,0}$ and a part $\dot{m}_{a,door}$ that is triggered by discrete door opening events ($\delta$):

$$\dot{m}_{a,in} = \dot{m}_{a,0} + \dot{m}_{a,door}\delta \tag{12}$$

The maximal air flow rate $\dot{V}_0$ is slowly degraded as the ice forms. This degradation rate is simplified with the following relation:

$$\frac{d\dot{V}}{dt} = -k_{fr}\dot{m}_{fr} \tag{13}$$

where the air flow degradation rate is much higher when the critical frost mass ($m_{fr,critical}$) is reached:

$$k_{fr} = \begin{cases} k_{fr,1} & \text{if } m_{fr} <= m_{fr,critical} \\ k_{fr,2} & \text{if } m_{fr} > m_{fr,critical} \end{cases} \tag{14}$$

Lastly, the degradation of the cooling capacity due to air flow degradation ($\eta_e$) can be defined as the ratio of the air flow of the frosted evaporator ($\dot{V}$) and the evaporator without frost ($\dot{V}_0$). The derivative of the degradation ratio can be defined as

$$\dot{\eta}_e = -\frac{k_{fr}}{\dot{V}_0}\dot{m}_{fr} \tag{15}$$

Air flow of the opened cabinet door was evaluated with the use of infiltration air load equation, suggested in [28]:

$$\dot{m}_{a,door} = 0.221A\rho_{a,ref}\left(1 - \frac{\rho_{a,s}}{\rho_{a,ref}}\right)^{0.5}(gH)^{0.5}F_m \tag{16}$$

$$F_m = \left(\frac{2}{1 + \left(\frac{\rho_{a,ref}}{\rho_{a,s}}\right)^{1/3}}\right)^{1.5} \tag{17}$$

where $A$ is a non-blocking area of the refrigeration shelves, $g$ is the gravitational constant, $H$ is the height of the non-blocking area, and $\rho_{a,ref}$ and $\rho_{a,s}$ denote air densities in refrigerator and in the store, respectively.

Since, ice formation measurements were not available, some extra assumptions were needed to determine ice formation model. Assumption was made that nominal air exchange of the closed cabinet ($\dot{m}_{a,0}$) is three times smaller than $\dot{m}_{a,door}$. Moreover, it was assumed that critical degradation rate is much higher than degradation in normal operation ($k_{fr,2} = 5k_{fr,1}$). Finally, the constant relation $\frac{k_{fr,1}}{\dot{V}_0}$ was defined on the basis of the observed degradation of valve opening that was evaluated during the long-term operation within the shop's closing hours. Several valve opening trends were averaged to determine small but constant declination of valve opening that is needed to guarantee complete evaporation of the refrigerant within the frosted evaporator's coil.

## 2.2. Discrete event model of a display case

Whilst the refrigeration system is in operation, various situations occur that are of a discrete nature. A discrete model of refrigeration is introduced to supplement the dynamical refrigeration model with typical everyday operating events. Some parameters of the discrete model were taken from the observed store and the others were estimated based on our experience.

*2.2.1. Customer behaviour*

Customers arrive and take products from the refrigerator according to the time and day of the week. Since we do not have historical data from the analysed store, we selected these parameters according to preliminary measurements and our experience. In the weekdays, we assume that customers arrive with an exponentially distributed interarrival time with mean $\lambda = 1/6\ \mathrm{h}^{-1}$, i.e. at a rate of 6 customers per hour. The costumer arrival rate is higher in peak hours (3–8 PM) and on Sundays ($\lambda = 1/9\ \mathrm{h}^{-1}$), and lower on weekday evenings (8–9 PM), $\lambda = 1/3\ \mathrm{h}^{-1}$. The schedule of customer arrival rates, depending on the time and the day of the week, is given in Fig. 3.

When a customer takes a product, the refrigerator's door is open for an exponentially distributed time of 10 s ($\lambda = 0.1\ \mathrm{s}^{-1}$) and the quantity of product items within the refrigerator is decreased. For every product taken, the core and surface masses are decreased by, respectively, 0.5 kg (core weight of a single product) and 0.057 kg (surface weight of a single product).

Block *source1* generates the entities (customers) with rates defined by the schedule in Fig. 3. The *queue1* represents the waiting queue of customers waiting to open the door and take the product (we assume that only one customer can open the door at the same time). The *RefOpTake* block represents the action of opening the door and defines how long the door is open by each customer. It implements also the mass decrease. The last block (*sink1*) disposes the entities.

Door openings also influence the heat transfer of the refrigerator. This is included with the following term, which is added to the model introduced in the previous section.

$$\dot{Q}_{door} = \dot{m}_{a,door}(h_{a,s} - h_{a,ref})\delta. \tag{18}$$

Here, $h_{a,s}$ is the enthalpy of the incoming air, $h_{a,ref}$ is the enthalpy of the refrigerated air. $\delta$ is a door opening variable that considers the status of the door according to the discrete-event model describing the customers' arrivals, as shown in Fig. 4.

$$\delta = \begin{cases} 1 & \text{if the door is open} \\ 0 & \text{if the door is closed} \end{cases} \tag{19}$$

*2.2.2. Filling with the products*

To define how full the refrigerator is, we introduce a variable *Fullness* (*Fullness* = 1 means full and *Fullness* = 0 means empty). When *Fullness* is below a certain threshold, the refrigerator is refilled with new product item entities. This threshold is defined randomly for each refrigerator loading through a triangular distribution $T(min, max, mode)$ with mode $Thr_m = 0.4$, i.e. $Thr = T(Thr_m - 0.2, Thr_m + 0.2, Thr_m)$.

Also, the time for refilling is presumed to be variable, however this should depend on how many products have to be refilled. This was implemented with a triangular distribution, which depends on $Thr : T(2, 2 + 6(1 - Thr), 8)$ mins.

We assume that the temperature of the incoming entities is not always the same. We consider it to be distributed in the range defined by $T(-20, -16, -19)$ °C.

| Sun | Mon | Tue | Wed | Thu | Fri | Sat | Start | End | Value |
|---|---|---|---|---|---|---|---|---|---|
| ☐ | ✓ | ✓ | ✓ | ✓ | ✓ | ✓ | 8:00 AM | 3:00 PM | 6 |
| ☐ | ✓ | ✓ | ✓ | ✓ | ☐ | ☐ | 3:00 PM | 8:00 PM | 9 |
| ☐ | ✓ | ✓ | ✓ | ✓ | ☐ | ☐ | 8:00 PM | 9:00 PM | 3 |
| ☐ | ☐ | ☐ | ☐ | ☐ | ✓ | ✓ | 3:00 PM | 9:00 PM | 9 |
| ✓ | ☐ | ☐ | ☐ | ☐ | ☐ | ☐ | 8:00 AM | 1:00 PM | 6 |

**Fig. 3.** Schedule of customer arrivals, defined as arrivals per hour.

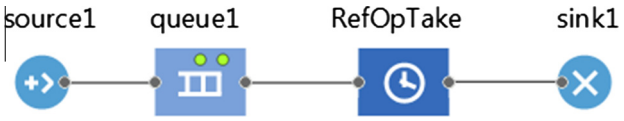


**Fig. 4.** DE model of door openings and total mass decrease.

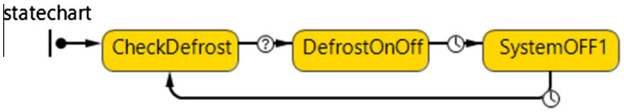


**Fig. 5.** Statechart connecting the dynamical part of the refrigeration model and the discrete defrosting events.

During the refilling time, the refrigerator's door is open. The influence on the heat transfer is considered similarly to what was previously done by Eq. (18).

*2.2.3. Defrosting*

In order to increase the overall efficiency of the refrigerator, the evaporator has to be defrosted periodically. A common practice in commercial refrigeration systems is to define a defrosting schedule that defrosts the evaporator's coils. The coils are defrosted with the use of a heater that actively removes the formed frost. In our case, the defrost heaters are turned on discretely during defrosting periods and are considered to operate at constant power (i.e. $\dot{Q}_h = 3100\ \mathrm{W}$).

Discrete defrosting events are included in the model with the use of the statechart depicted in Fig. 5. When the initial condition is triggered by the scheduler, the refrigeration system is turned off and the system goes into the defrosting state (*DefrostOnOff*). When the defrosting is finished (after 22.5 min), the heater is turned off and the system moves to the state that delays the activation of the refrigeration system for 4.2 min (*SystemOFF1*).

*2.3. Model extension to the store-wide refrigeration system*

In order to extend the analysis to the level of a complete store where several parallel display cases are present, additional display cases need to be introduced. The identified display case model is implemented as an agent model in the AnyLogic software package. This way, several display cases can be easily replicated, where the identified model acts as a agent basis. Individual agents (display cases) are then initialised with a variation of the distinctive model parameters.

For demonstration purposes, only low temperature display cases are considered. The display cases are assumed to have the same refrigeration characteristics, whilst the food characteristics and customers activity vary, as shown in Table 2.

## 3. Optimisation analysis

With the developed model, alternative optimisation actions can be directly compared. In this way, an acceptable action that promises enough energy related savings can be identified. The optimisation scenarios are divided into two main parts. The first part considers the optimisation of the applied defrost-scheduling strategy, and the second part evaluates the savings of different energy optimisation actions that can be performed or influenced by the display case owners.

**Table 2**
Parameters of the store's display cases.

| | dc. 1 | dc. 2 | dc. 3 | dc. 4 | dc. 5 | dc. 6 |
|---|---|---|---|---|---|---|
| Food type | Ice cream | Vegetable | Vegetable | Meat | Meat | Fish |
| $c_{Pc}$ | 2750 | 1900 | 1900 | 2500 | 2500 | 2150 |
| Maximal number of products | 250 | 350 | 350 | 300 | 300 | 200 |
| Mass of one item | 0.5 | 0.45 | 0.45 | 0.65 | 0.65 | 0.25 |
| Customer arrival rate – *min* | 0.05 | 0.13 | 0.06 | 0.13 | 0.06 | 0.02 |
| Customer arrival rate – *max* | 0.12 | 0.22 | 0.14 | 0.22 | 0.14 | 0.08 |
| Customer arrival rate – *peak* | 0.2 | 0.3 | 0.2 | 0.3 | 0.2 | 0.15 |

### 3.1. Optimisation objectives

The key objective is to minimise the total energy cost. This can be evaluated as the integral over the simulated time $T$:

$$C_{tot} = \int_0^T (P_{ref} + \dot{Q}_h) \cdot c_e dt \tag{20}$$

where $P_{ref}$ is the power used by the compressor (see Eq. (10)), $\dot{Q}_h$ is the defrost heater power, and $c_e$ is assumed to be the time-dependent energy tariff, i.e. 0.04391 € per kW h from 22:00 to 06:00 every weekday and 0.07929 € per kW h every weekday from 06:00 to 22:00 and during the weekends.

Cost optimisation directly influences the quality of the refrigeration. Therefore, special focus is needed to monitor the food quality. Food quality decay can be determined by many environmental factors, but out of all of these, temperature is the most influential. As proposed in [21], the food quality indicator can be calculated as follows:

$$q_{food,loss} = \frac{e^{\frac{T_c - T_{ref}}{z}} \cdot 100}{D_{T,ref}} \tag{21}$$

where $z$ is the product temperature sensitivity indicator and $D_{T,ref}$ is the time for loss of quality at $T_{ref}$. The reference temperature for frozen products is normally $T_{ref} = -18\,^{\circ}C$, but should be individually set in accordance with the HACCP. In our case we use $z = 20\,^{\circ}C$ and $D_{T,ref} = 125$ days to describe the property of the refrigerated items. The current food quality index $Q_{food,loss}$ can be evaluated as an integral of the food decay ratio, in which a uniform quality of the product items in the refrigerator is observed. The additional assumption is made that newly added items have 100% quality and the overall food quality is averaged with the older items in the refrigerator.

Another objective that needs to be monitored is the power consumption peak. High power peaks needs to be avoided in normal operating conditions, as this guarantees a stable power supply and low energy prices. To quantify the difference between alternative simulation runs, a power peak index $P_{max}$ is introduced. This index is defined as the maximal power consumption in the complete simulation run:

$$P_{max} = max(P_{ref} + \dot{Q}_h) \tag{22}$$

### 3.2. Defrost-schedule optimisation

The frost formed on the coils of the evaporator decreases the cooling capacity, which is directly reflected in a higher operating cost. But the defrosting actions are also very energy demanding, as they require extra energy from the heater and this extra energy needs to be eventually removed from the display case. Therefore, too frequent defrosting is expected to increase the overall energy consumption and at the same time significantly affect the food quality. The main question is when and how often should defrosting actions be scheduled for normal operating conditions.

The analysis was based on a systematic variation of the defrosting schedule. For each case, either a 30-day simulation run (single display case schedule) or a 7-day simulation run (store-wide schedule) was performed. Moreover, 30 repetitions per case were conducted, to take into account the model's randomness. For each run, the distribution of the operating costs and monthly quality decay were observed and compared.

#### 3.2.1. Display case defrost schedule optimisation

In this section, the optimisation results, performed on a single display case, are presented. In the first step, the one defrost per day scenario was analysed. It was assumed that the defrosting procedure occurs at the same time of day. The mean and two sigma data variability of the analysis results are shown in Fig. 6a. As

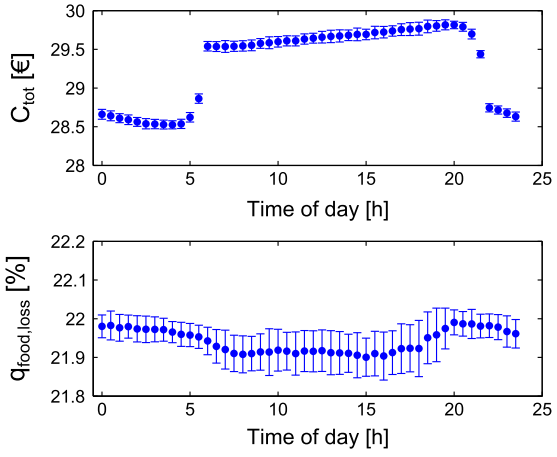


(a) One defrost per day: importance of scheduled defrost time

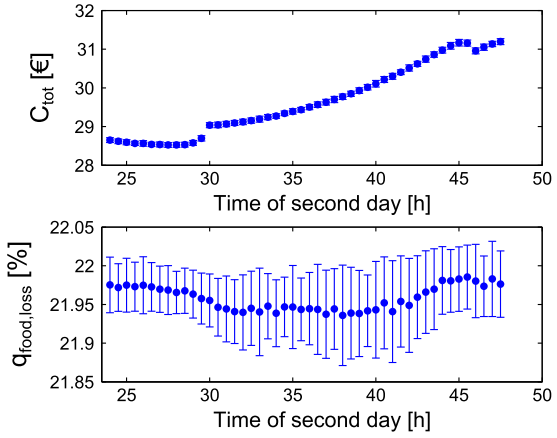


(b) Two defrosts per two days: importance of second defrost time (first defrost is scheduled at 4 AM of the first day)

**Fig. 6.** Single display case defrost schedule optimisation.

expected it is better to defrost during the time of the low energy tariff, but this yields a just slightly higher quality decay of the product items (which is not critical in this case). From the presented results it can be concluded that an early morning defrosting scenario can be found as the most optimal.

In the next step, a two-day defrosting scenario was tested, where the schedule defined for two consecutive days is repeated thereafter. The defrost schedule for the first day was fixed at the previously found optimal setting (i.e. 4 AM) and the defrost schedule for the second day was systematically varied. The results, shown in Fig. 6b, suggest that there is no need to use a two-day defrosting schedule, as an early morning scenario is again found to be optimal.

### 3.2.2. Store-wide defrost schedule optimisation

A store-wide defrost schedule was constructed with the introduction of two new parameters: $t_{start}$ and $t_d$, where $t_{start}$ indicates the defrost schedule start of the first display case (dc. 1) and $t_d$ denotes the defrost schedule delays for the remaining display cases. The starting time of the defrost schedule for the $n$th display case can be therefore formulated as $t_s + (n-1)\cdot t_d$. With the systematic variation of the both schedule parameters, alternative schedules were validated.

Fig. 7 shows the relevant performance indicators for different defrost start times ($t_{start}$) and three alternative time delays ($t_d$). Note, that the represented indicators are averaged over several store display cases with diverse physical properties (see Table 2) and therefore their absolute values cannot be directly compared with the results for a single display case. As expected, it is optimal to defrost all the display cases in the morning with the previously found optimal defrost schedule (i.e. 4 AM). If defrosts of different display cases are intended to be delayed, then the defrost time of the first display case needs to occur earlier in the morning/night.

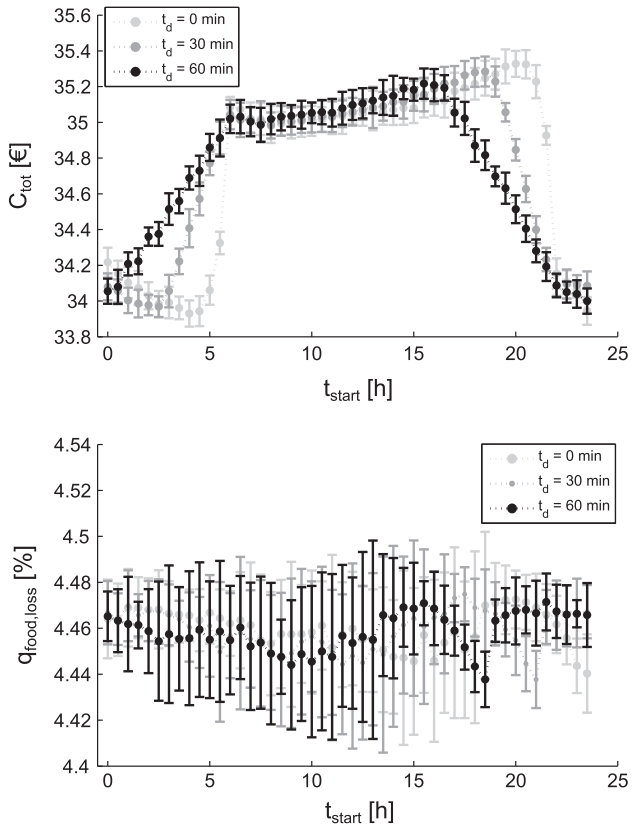


**Fig. 7.** Influence of the first display case defrost start time.

Defrosts that are scheduled during the shop's opening time are expected to cause more intensive food quality variations. The reason for this is the additional display case disturbances, such as door openings by the customers and shop employees.

A defrost scenario with no time delay between the display causes high peaks of the refrigerant flow. This must be compensated by an increased activity of the compressor pack. To cover all these refrigerant peaks, the compressor needs to be over-specified. Moreover, the synchronised use of defrost heaters causes a high power peak, which is additionally prolonged by the power peak of the compressor-pack. If the compressor activity is to be distributed more evenly, and if the electrical power peaks are to be avoided, then the indicator of maximal power $P_{max}$ needs to be minimised.

The defrost schedule analysis according to the power peaks is shown in Fig. 8. The results indicate that no matter when the defrost procedure starts, it is important that at least a 30 min delay between the defrosts is applied.

To determine the optimal store-wide defrost schedule that would satisfy both criteria ($C_{tot}$ and $P_{max}$), a unified performance criterion is selected:

$$J_{opt} = J_{Ctot} + J_{Pmax} \tag{23}$$

Each element of the optimisation criterion represents the normalised equivalent of the elementary criteria in the range of 0 and 1. Their definitions are

$$J_{Ctot}(t_d, t_{start}) = \frac{C_{tot}(t_d, t_{start}) - min(C_{tot})}{max(C_{tot}) - min(C_{tot})}, \tag{24}$$

$$J_{Pmax}(t_d, t_{start}) = \frac{P_{max}(t_d, t_{start}) - min(P_{max})}{max(P_{max}) - min(P_{max})}. \tag{25}$$

Here, a complete space search was performed in advance of evaluating the objectives $C_{tot}$ and $P_{max}$ for alternative combinations of $t_d$ and $t_{start}$ with step sizes of 0.125 h and 0.5 h, respectively. On the basis of these simulation results, a minimal and maximal value of each partial objective was found, and used to weight their importance.

The unified performance criteria $J_{opt}$ for whole observed space is shown in Fig. 9. In this way, the schedule with the optimal values of cost and maximal current criteria was found. It is most viable to start defrosting the first display case at 1:30 AM and delay defrosting each following display case by 37.5 min.

### 3.3. Benefits of energy optimisation measures

Several approaches can be taken to optimise the everyday running costs of the refrigeration systems. But these approaches can directly or indirectly influence the employees work-load, customer behaviour, etc., and therefore it is good to know what to expect from such a measure prior to making changes.

In this study we analyse the following actions: (i.) increase of a display case temperature, (ii.) decrease of the store's temperature, (iii.) decrease in the door opening time, (iv.) maximal food-load of the display case, and (v.) display case refilling threshold. The expected benefits of these actions are analysed and compared, where the cost savings and food quality degradation are the main performance measures. For each specific action considered, a systematic parameter variation was performed. For each tested value of the parameter, a 30-day simulation run was evaluated with 30 repetitions for each case.

The simulation results are plotted in Fig. 10 and the optimisation measures effects are linearised for both performance indexes (i.e. $C_{tot}$ and $q_{food,loss}$). The linearised slopes of the energy

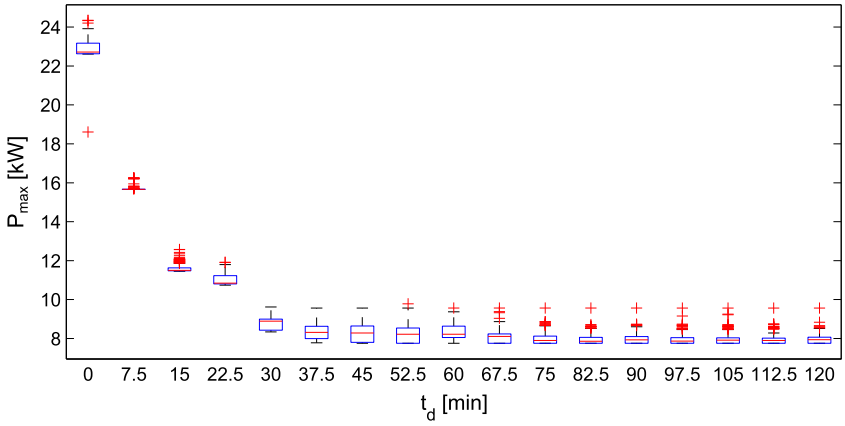


**Fig. 8.** Influence of defrost schedule delay time on maximal power peak (for all $t_{start}$ values).

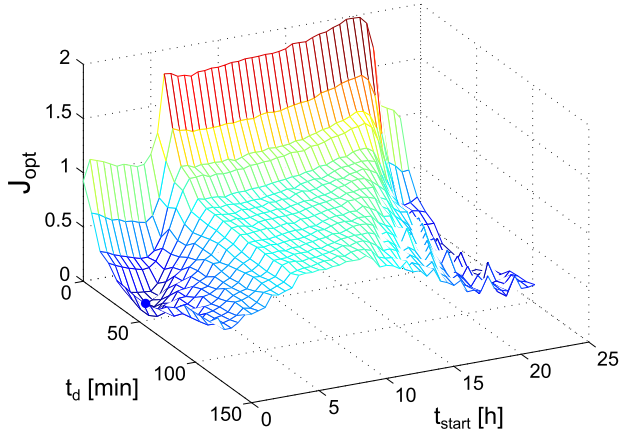


**Fig. 9.** Defrost schedule optimisation results (optimal performance index at $t_d = 37.5$ and $t_{start} = 1.5$).

optimisation measures are shown in Table 3, which offers a direct comparison of the expected benefits for the considered measures.

### 3.3.1. Display case temperature

The display case temperature has a significant influence on the running refrigeration costs. The selected temperature usually directly follows the HACCP standard for the refrigerated food. Moreover, some temperature offset is usually needed to guarantee the needed food quality for all operating conditions.

The analysis of the display case temperature shows a significant relation with costs (see Fig. 10a) and also the quality decay ratio is significantly increased. A cost optimisation approach where the refrigeration temperature is set as close as possible to the HACCP standard is therefore suitable only for quickly sold items and items that do not quickly deteriorate.

### 3.3.2. Store temperature

The temperature of the air surrounding the display case can be influenced by the store owners. On the one hand, the air temperature of the complete store can be decreased. Note that this may directly yield higher HVAC operating costs. On the other hand, the positioning of the display cases plays an important role that directly influences the temperature around the display cases. This effect can even be intensified with special rooms for refrigerators or with some other air blocking barriers/solutions.

As shown in Fig. 10b, an increased air temperature of the store drastically effects the operating costs of the refrigerators. Simulation shows that decreasing the outside temperature by 1 °C causes savings in the range of 2.38%. Decreasing the store's temperature also affects slightly the slower degradation of the food quality.

### 3.3.3. Door openings

Too frequent door openings significantly increase the energy losses, increase the frost formation, and increase the cabinet temperature. All of this is directly reflected in the higher operational costs and lower product quality. The store owners have the possibility to motivate the customers and employees to limit the door opening time, or to install auto-closing mechanisms if there are significant occasions when customers forget to close the doors. Moreover, the maintenance of the door needs to be regular to decrease the unwanted air flows through the closed doors.

The results in Fig. 10c show that if the mean opening time of the doors can be reduced by ten seconds, this can result in a 1.2% decrease in operating costs. Therefore, to some extent, it is worth motivating and helping the customers to shorten their reach-in time. But if this time is short already, such an action can act as a demotivation factor for the customers and bring no real benefit.

### 3.3.4. Maximal food mass and display case refilling strategy

The mass of the food in the refrigerator can play a significant role in refrigeration operation. A small food mass can cause high temperature variations in the case of disturbances. This will be reflected in faster food quality degradation. The average mass of food in the refrigerator can be directly influenced by the maximal food mass that is regularly loaded into the refrigerator. Also, the refrigeration loading strategy can play an important role, as frequent food loading will guarantee a large food mass and small food quality degradation ratio, but the energy losses will be significantly higher due to the increased door opening time.

The change of the maximal food-load limit shows (see Fig. 10d) that there is expected a relatively small increase in the operation costs, i.e. a 0.1% operating cost increase for increase of maximal mass load for 100 kg. There is also some decrease in food quality degradation ratio, but not as big as expected: for a 100 kg higher food-load level, there is expected an increase of the food quality degradation ratio of 0.3%.

To test how often the display cases should be refilled with fresh product items, we have systematically varied the distribution mean of the minimal product threshold in the refrigerator. Moreover, it is expected that the shop employees would stick more firmly to the tested measure, therefore the refilling distribution is additionally tightened (the deviation from the mean is changed from 0.2 to 0.025; $Thr = T(Thr_m - 0.025, Thr_m + 0.025, Thr_m)$). The

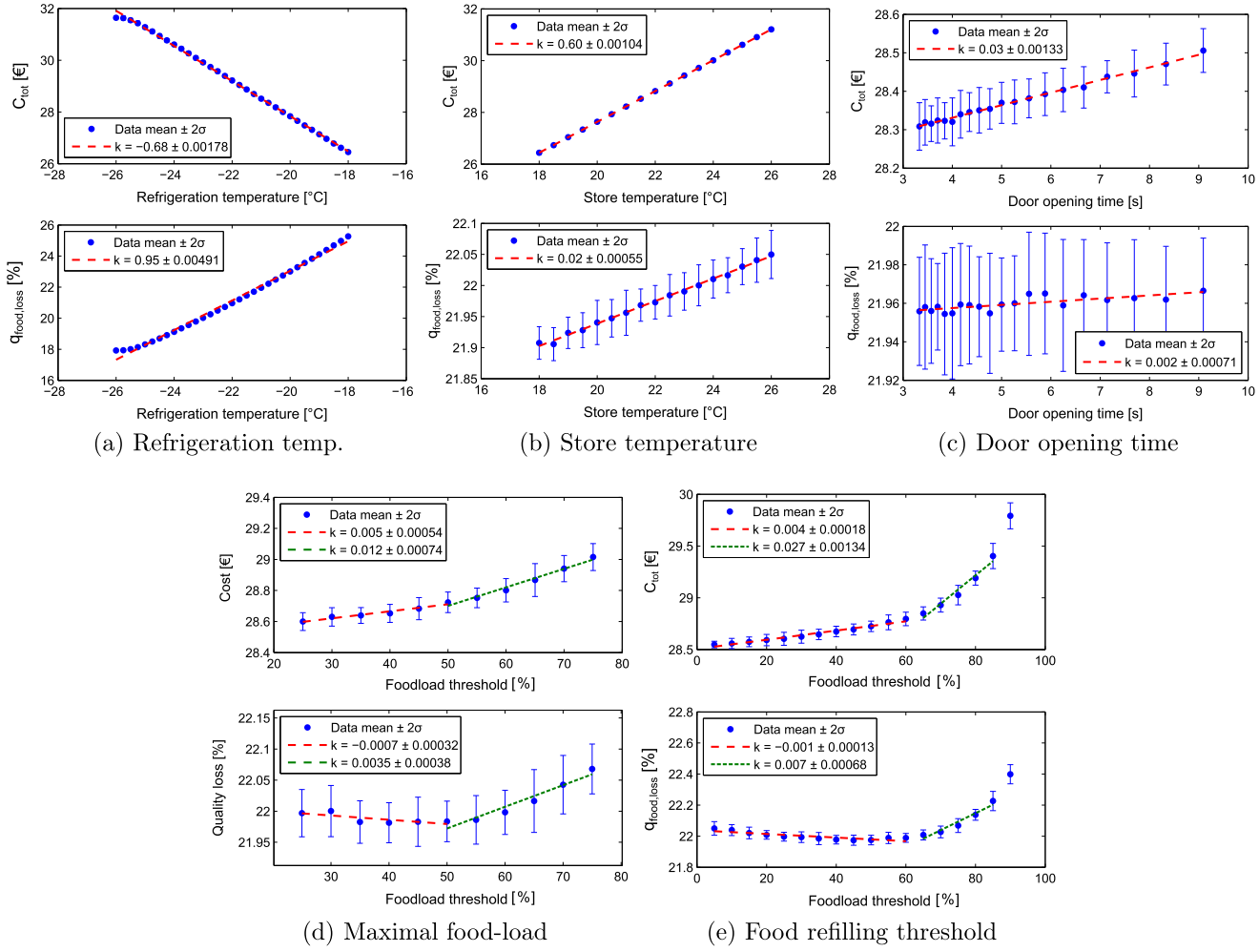


(a) Refrigeration temp. (b) Store temperature (c) Door opening time

(d) Maximal food-load (e) Food refilling threshold

**Fig. 10.** Benefits of energy optimisation measures.

**Table 3**
Comparison of the energy optimisation measures (italicised fields indicate negative correlation between the measure and specific performance indicator).

| Action | Range | Unit | Savings in € | | Savings in % of nominal operating cost (i.e. 28.52€) | | Quality decay | |
|---|---|---|---|---|---|---|---|---|
| | | | $k$ (€/unit) | $\pm CI_{95\%}$ ($10^{-4}$ €/unit) | $k$ (%/unit) | $\pm CI_{95\%}$ ($10^{-4}$ %/unit) | $k$ (%/unit) | $\pm CI_{95\%}$ ($10^{-4}$ %/unit) |
| Refrigeration temp. | [−26, −18] | °C | *−0.68* | *18* | *−2.38* | *63.1* | 0.95 | 49 |
| Store temp. | [18,26] | °C | 0.60 | 10 | 2.10 | 35.1 | 0.018 | 5.5 |
| Door opening time | [3.3,28.5] | s | 0.033 | 13 | 0.12 | 45.6 | 0.0016 | 7.0 |
| Max. food-load (i.) | [100,200] | kg | 0.0012 | 1.0 | 0.004 | 3.5 | *−0.0028* | *0.64* |
| Max. food-load (ii.) | [200,300] | kg | 0.00083 | 1.3 | 0.003 | 4.6 | *−0.0015* | *0.50* |
| Refilling threshold (i.) | [5,65] | % | 0.0044 | 1.8 | 0.015 | 6.3 | *−0.0012* | *1.3* |
| Refilling threshold (ii.) | [65,85] | % | 0.027 | 13 | 0.095 | 45.6 | 0.011 | 6.8 |

results in Fig. 10e show that too frequent refiling scenarios should be avoided (above 65% of food-refiling threshold). To some extent some cost reduction is expected if the food loading limit is decreased, but this will also make for a slightly quicker food quality decay.

## 4. Conclusions

In this paper, a framework for analysing and optimising the operation of display cases has been presented. Our approach allows us to validate the benefits of potential optimisation actions prior to their implementation. Moreover, the multi-objective analysis guarantees that several objectives (i.e. operation costs, quality degradation and power peaks) can be simultaneously considered.

The analysis is based on the developed refrigeration model, which integrates the temperature dynamics and discrete events that usually result from human interaction. This way, a considered optimisation activity can be extended even to the level of human behaviour. Several model simplifications were made in order to simplify the model instantiation, that should be based on measured refrigeration data, the specifications of the equipment and food items, and on-site observations. The simplicity of the model allowed us to quickly scale the problem to the store level, as was shown in the store-wide schedule optimisation problem. The considered case study has shown how alternative optimisation actions can be easily evaluated and compared. The list of actions could be even further extended if some specific optimisation actions were in question.

## Acknowledgements

The presented research was performed within the projects supported by the Slovenian Research Agency (Grants L2-5476 and P2-0001) and ERASMUS + traineeships program.

## References

[1] M. Umberger, I. Humar, Energy Savings of Refrigerators in Shopping Centers with Adaptive Control and Real-Time Energy Management Systems, Tech. rep., University of Ljubljana, Faculty of Electrical Engineering, 2012.
[2] J. Evans, E. Hammond, A. Gigiel, A. Fostera, L. Reinholdt, K. Fikiin, C. Zilio, Assessment of methods to reduce the energy consumption of food cold stores, Appl. Therm. Eng. 62 (2) (2014) 697–705.
[3] R. Chandrasekharan, C. Bullard, Analysis of Design Tradeoffs for Display Case Evaporators, Tech. rep., ACRC, University of Illinois at Urbana-Champaign, 2004.
[4] Y. Ge, S. Tassou, I.D. Santosa, K. Tsamos, Design optimisation of $CO_2$ gas cooler/condenser in a refrigeration system, Appl. Energy 160 (2015) 973–981.
[5] L. Cecchinato, M. Corradi, S. Minetto, Energy performance of supermarket refrigeration and air conditioning integrated systems, Appl. Therm. Eng. 30 (2010) 1946–1958.
[6] T. Hovgaard, L. Larsen, K. Edlund, J. Jørgensen, Model predictive control technologies for efficient and flexible power consumption in refrigeration systems, Energy 44 (2012) 105–116.
[7] H. Weerts, S. Shafiei, J. Stoustrup, R. Izadi-Zamanabadi, Model-based predictive control scheme for cost optimization and balancing services for supermarket refrigeration systems, in: Proceedings of the 19th IFAC World Congress, 2014, pp. 975–980.
[8] K. Proelss, G. Schmitz, Modeling of frost growth on heat exchanger surfaces, Vienna, Austria, in: Proceedings of the 5th Modelica Conference, 2006.
[9] J. Xie, X.-H. Qu, J.-Y. Shi, D.-W. Sun, Effects of design parameters on flow and temperature fields of a cold store by CFD simulation, J. Food Eng. 77 (2006) 355–363.
[10] M. Mohanraj, S. Jayaraj, C. Muraleedharan, Applications of artificial neural networks for refrigeration, air-conditioning and heat pump systems—a review, Renew. Sustain. Energy Rev. 16 (2012) 1340–1358.
[11] J.-S. Chou, Y.-C. Hsu, L.-T. Lin, Smart meter monitoring and data mining techniques for predicting refrigeration system performance, Expert Syst. Appl. 41 (2014) 2144–2156.
[12] A. Kusiak, G. Xu, Modeling and optimization of HVAC systems using a dynamic neural network, Energy 42 (2012) 241–250.
[13] L. Zhao, W. Cai, X. Ding, W. Chang, Model-based optimization for vapor compression refrigeration cycle, Energy 55 (2013) 392–402.
[14] T. Nunes, J. Vargas, J. Ordonez, D. Shah, L. Martinho, Modeling, simulation and optimization of a vapor compression refrigeration system dynamic and steady state response, Appl. Energy 158 (2015) 540–555.
[15] Y. Ge, S. Tassou, Performance evaluation and optimal design of supermarket refrigeration systems with supermarket model "SuperSim"* part I: model description and validation, Int. J. Refrig. 34 (2011) 527–539.
[16] K. Vinther, H. Rasmussen, R. Izadi-Zamanabadi, J. Stoustrup, A. Alleyne, A learning based precool algorithm for utilization of foodstuff as thermal energy storage, in: IEEE International Conference on Control Applications, 2013, pp. 314–321.
[17] S.E. Shafiei, H. Rasmussen, J. Stoustrup, Modelling supermarket refrigeration systems for demand-side management, Energies 6 (2013) 900–920.
[18] L.N. Petersen, H. Madsen, C. Heerup, ESO2 Optimization of Supermarket Refrigeration Systems—Mixed Integer MPC and System Performance, Tech. rep., Technical University of Denmark, Department of Informatics and Mathematical Modelling, 2012.
[19] M. Ducoulombier, A. Teyssedou, M. Sorin, A model for energy analysis in supermarkets, Energy Build. 38 (2006) 349–356.
[20] E. Kremers, J. Durana, O. Barambones, Emergent synchronisation properties of a refrigerator demand side management system, Appl. Energy 101 (2013) 709–717.
[21] J. Cai, J. Stoustrup, B.D. Rasmussen, An active defrost scheme with a balanced energy consumption and food quality loss in supermarket refrigeration systems, in: Proceedings of the 17th IFAC World Congress, 2008, pp. 9374–9379.
[22] T. Green, R. Izadi-Zamanabadi, R. Razavi-Far, H. Niemann, Plant-wide dynamic and static optimisation of supermarket refrigeration system, Int. J. Refrig. 38 (2014) 106–117.
[23] AnyLogic, Multimethod Simulation Software <www.anylogic.com>.
[24] H. Boysen, $k_v$: What, Why, How, whence?, Tech. rep., Danfoss, 2011.
[25] Danfoss, Electrically Operated Expansion Valve Types AKV 10, AKV 15 and AKV 20, Data sheet, 2012.
[26] M. Skovrup, A. Jakobsen, B. Rasmussen, S. Andersen, CoolPack v1.5, Technical University of Denmark, 2012. available: <http://en.ipu.dk/Indhold/refrigeration-and-energy-technology/coolpack.aspx>.
[27] D.L. Da Silva, Frost formation on fan-supplied tube-fin evaporators: a visual and numerical analysis, in: International Refrigeration and Air Conditioning Conference, 2012.
[28] American Society of Heating, Refrigeration and Air-Conditioning Engineers, Refrigeration load, in: 2002 ASHRAE Refrigeration Handbook, American Society of Heating, Refrigeration and Air-Conditioning Engineers, Atlanta, GA, 2002.